New laboratory bounds on the stability of the electron

Y. Aharonov,[1,4] F. T. Avignone III,[1] R. L. Brodzinski,[2] J. I. Collar,[1] E. García,[3] H. S. Miley,[2] A. Morales,[3] J. Morales,[3] S. Nussinov,[4] A. Ortiz de Solórzano,[3] J. Puimedón,[3] J. H. Reeves,[2] C. Sáenz,[3] A. Salinas,[3] M. L. Sarsa,[3] and J. A. Villar[3]

[1] *University of South Carolina, Columbia, South Carolina 29208*

[2] *Pacific Northwest Laboratory, Richland, Washington 99352*

[3] *Laboratorio de Física Nuclear, Universidad de Zaragoza, 50009 Zaragoza, Spain*

[4] *Tel Aviv University, Tel Aviv 69978, Israel*

(Received 13 February 1995)

A set of two natural abundance Ge detectors of 1.1 kg each, located in the Homestake mine, and one small, 0.253 kg, Ge detector operating in the Canfranc railway tunnel in Spain, have been used to obtain bounds on the stability of the electron against the decay modes $e^- \to \gamma\nu_e$ and $e^- \to \nu_e\nu_e\bar{\nu}_e$. The bounds on the mean lives are $\tau(\gamma\nu_e) > 3.7(2.1) \times 10^{25}$ yr 68%(90%) C.L. and $\tau(\nu_e\nu_e\bar{\nu}_e) > 4.3(2.6) \times 10^{23}$ yr, 68% (90%) C.L., which are at present the most stringent laboratory limits for these decays. The theoretical controversy concerning the relevance of such data to fundamental tests of charge conservation is also considered.

PACS number(s): 13.35.−r, 11.30.−j, 14.60.Cd

I. INTRODUCTION

In the context of gauge field theories, the invariance of the Lagrangian $\mathcal{L}$ under a given gauge transformation corresponds to the conservation of some specific type of "charge." In some grand unified theories, for example, terms appear in $\mathcal{L}$ which break the global gauge invariance associated with baryonic charge (baryon number) leading to proton decay at some level [1,2]. In the electroweak sector, the local gauge invariance of the Lagrangian corresponding to the equations of quantum electrodynamics dictates strict electric charge conservation and a massless photon. Accordingly, in the context of this class of theories, we do not expect electrons to decay, because there is no lighter charged lepton, and the decay into photons and/or neutrinos requires the violation of charge conservation. Nevertheless, to neglect searches for the unexpected is tantamount to assuming *a priori* that our current understanding of particle physics is complete and correct. It is of paramount importance to test each conservation law to the best of our experimental ability.

Experimental tests of charge conservation via the search for spontaneous x rays or 255 keV γ rays from the decay modes $e^- \to \nu_e\nu_e\bar{\nu}_e$ and $e^- \to \gamma\nu_e$, respectively, have a long history well covered in the literature [3–9]. In addition, a number of detailed theoretical discussions of electric charge conservation in the context of renormalizable gauge field theories appear in the literature [10–13]. An essential point is that the local gauge invariance of the Lagrangian of quantum electrodynamics (QED) stems from the massless gauge bosons and guarantees via Noether's theorem that the corresponding charge is exactly conserved. In fact, a finite photon mass alone would not destroy exact charge conservation; this would also require terms in the Lagrangian that destroy global as well as local gauge invariance [2].

The search for the decay of the electron as an experimental test of charge conservation was first suggested by Feinberg and Goldhaber [9]. Recently, however, there have been some reasonably cogent theoretical arguments against the use of x-ray and γ-ray data to search for the decay of the electron [14–17]. These arguments, however, require certain fundamental assumptions in the interpretation of infinite amplitudes rendering the conclusions model dependent. In the next section, we discuss the relevant issues involved in the arguments of Okun and Zeldovich [14], of Okun [15], of Suzuki [16], and of Tsypin [17].

This paper reports new limits on the mean life of the electron by using the data of the background spectra obtained with two sets of germanium detectors: A pair of twin Ge detectors of about 1.1 kg each, operating 1438 m underground in the Homestake Laboratory [4000 meters of water equivalent (mwe)], South Dakota, and one small 0.253 kg Ge detector located in the Canfranc Laboratory, Aragonese Pyrenees, Spain, located 260 meters underground (675 mwe). The results are by-products of ongoing investigations on the double β decay of ^{76}Ge and on the search for particle dark matter in the galactic halo. Sections III and IV describe the experimental procedure and results.

II. THEORETICAL CONSIDERATIONS

Since charge conservation and massless photons are both automatic consequences of standard QED and relate directly to gauge invariance, the unifying theme in modern quantum field theory, it is very important to test both with the best experimental sensitivity available.

A well known theorem by Weinberg [18] forbids the violation of electric charge conservation if the photon is exactly massless. The introduction of a charge-violating (CV) term, e.g., $\kappa\bar{\psi}_e \not{A}\psi_\nu$, into the Lagrangian to gener-

ate the process $e^- \to \gamma + \nu_e$, for example, violates gauge invariance; this in turn destroys renormalizability. In this case, the photon mass is no longer zero and is given by

$$m_\gamma = \kappa\Lambda \ , \tag{1}$$

where Λ is an appropriate momentum cutoff. Since charge conservation is directly correlated with the condition $m_\gamma = 0$, it is interesting to ask which constitutes the most sensitive test at the present time? More specifically we can ask the following: (1) Do the upper bounds on the photon mass already exclude charge violating decays at rates to which present experiments are sensitive $\{\Gamma(e^- \to \gamma\nu_e) \leq 10^{-25}\ \text{yr}^{-1}\}$? Because of the lack of cancellation between pre- and post-emission, a CV event is expected to be accompanied by strong emission of longitudinal photons. Indeed, as emphasized by Okun and Zeldovich [14], the amplitude for emitting a longitudinal photon in a CV decay is proportional to $e(\bar{E}_\gamma/m_\gamma)$, and the amplitude for emitting n longitudinal photons $\sim e^n(\bar{E}_\gamma/m_\gamma)^n$. This factor grows with n as long as $\bar{E}_\gamma \equiv$ "m_{eff}"$/n \gg m_\gamma$, where $\bar{E}_\gamma$ is the average photon energy, and "m_{eff}" is the total rest frame energy available for longitudinal photon emission. Intuitively, such an enhanced emission reflects the "shedding off" of the quasi-long-range longitudinal configuration of the screened Coulomb field:

$$\bar{E}(\vec{r}) = \frac{e\vec{r}}{r^3}e^{-m_\gamma r} \ .$$

The absorption of longitudinal photons in usual charge-conserving processes is on the other hand suppressed by the factor $m_\gamma/\bar{E}_\gamma$. Thus the very strong emission of longitudinal photons could "drain" energy from the other decay products, e.g., the transverse photon in the decay $e^- \to \nu_e + \gamma_T + \gamma_{l_1} + \gamma_{l_2} + \cdots$. This naturally stimulated another question: (2) Does the emission of longitudinal photons mask the signatures of CV decays?

The lack of an adequate theoretical framework in which CV decays can be interpreted makes it very difficult to give clear-cut, model-independent answers to the above questions. We, nevertheless, will explore such possibilities within the bounds of generally accepted theories. One can invoke the above mentioned Weinberg [18] theorem, which depends only on unitarity and Lorentz invariance, or the more heuristic relation given in Eq. (1) to suggest that the relevant dimensionless coupling constant for CV decay processes is

$$\kappa_{\text{eff}} \sim m_\gamma/\Lambda \ . \tag{2}$$

In this case we expect

$$\Gamma(e^- \to \nu_e + \gamma_T + \cdots) \cong (\kappa_{\text{eff}})^2 m_e \cong m_e(m_\gamma/\Lambda)^2 \ . \tag{3}$$

There exists a direct upper bound on the photon mass from measurements of the magnetic field at some of the moons of Jupiter at distances of $\sim 10^{12}$ cm from the planet corresponding to [19]

$$m_\gamma \leq 10^{-17}\ \text{eV} \ . \tag{4a}$$

Another bound was inferred from the existence of the galactic magnetic fields over coherence lengths of $\sim 10^{22}$ cm; this corresponds to [19]

$$m_\gamma \leq 10^{-27}\ \text{eV} \ . \tag{4b}$$

The lowest value of the cutoff, Λ, in Eq. (3) is the rest mass of the electron, $\Lambda \cong m_e$. For this value of Λ, and the two bounds on m_γ stated in Eqs. (4a) and (4b), the following decay rates are implied:

$$\Gamma(m_\gamma < 10^{-17}\ \text{eV}; e^- \to \nu_e + \gamma) < 10^{-18}\ \text{yr}^{-1} \tag{5a}$$

and

$$\Gamma(m_\gamma < 10^{-27}\ \text{eV};\ e^- \to \nu_e + \gamma) < 10^{-38}\ \text{yr}^{-1} \ . \tag{5b}$$

We note that (5a) would still allow decay rates in the experimentally accessible region.

An extensive effort to find more concrete answers to the above questions within a Lagrangian framework was made by Voloshin and Okun (VO) [11]. Using a specific Lagrangian model for the CV process, they summed the tree diagrams for longitudinal photon emission, and the corresponding tree-plus-loop diagrams. Their results expression for the CV decay rate given by

$$\Gamma(e^- \to \nu_e + \gamma_T + \gamma_T + \gamma_{l_1} + \cdots)$$

$$\sim \alpha\kappa^2 \exp\{-\alpha\Lambda^2/2\pi m_\gamma^2\}$$

$$\times \exp\{3(\alpha\text{“}m_{\text{eff}}\text{”}/4\pi m_\gamma)^{2/3}\} \tag{6}$$

is very striking. It realizes the general Weinberg theorem, $\Gamma(\text{CV}) \to 0$ when $m_\gamma \to 0$, in a very dramatic form. The Gaussian factor in Eq. (6), even for the lowest value of Λ, and the highest value of m_γ used in Eqs. (5), is $\exp\{-10^{45}\}$. In this scenario, the theory with a small m_γ "heals itself" by suppressing CV decays.

Apart from affecting the rate, the longitudinal photons will reduce the energy in the decay products, impeding direct observation of decays such as $e^- \to \nu_e + \gamma_T$+longitudinal photons. Instead of the expected sharp spectral line at $E_\gamma \cong m_e/2$, the energy would be reduced and the line severely broadened. This effect will be very dramatic if the specific dependence of the decay rate on the total energy available, "m_{eff}," of VO is indeed correct; this dependence is contained in the factor

$$\exp\left\{3\left(\frac{\alpha}{4\pi}\frac{\text{“}m_{\text{eff}}\text{”}}{m_\gamma}\right)^{2/3}\right\} \ .$$

The rest frame energy would approach the kinematical maximum, "m_{eff}"$\cong m_e$, leaving zero energy for the $\nu_e + \gamma_T$ system.

The electron decay of interest here does not occur in a vacuum, but rather in the K shell of a heavy atom, germanium ($Z = 32$). Another interesting question is whether or not the transverse photons from the subsequent x-ray transitions would still be observable. At first glance, one might expect that this signal would not be af-

fected, since the transition has a finite lifetime ($\sim 10^{-15}$ s). However, in the formalism of VO [11], the exponential dependence on "m_{eff}" expressed in the second exponential factor of Eq. (6), suggests that this will not be the case. The energy of the L-shell electrons are higher than that of the K-shell electrons by about 10 keV ($\sim 0.02 m_e$). The result is that L-shell electron decay is more likely by a factor of

$$\exp\left\{(0.02)\frac{2}{3}\left(\frac{\alpha}{2\pi}\frac{m_e}{m_\gamma}\right)^{2/3}\right\} .$$

Even for the higher bound, $m_\gamma < 10^{-17}$ eV, this factor is as large as $\exp\{10^{15}\}$. This implies that a single K-shell electron decay should be accompanied by the decay of all higher shell electrons, and in fact all higher energy electrons in the universe. This argument is related to that given by Tsypin [17]. A similar enhancement could be obtained by putting free electrons in repulsive potentials.

The analysis of Voloshin and Okun [11] makes several rather strong assumptions in the interpretation of the results of their calculations. They found that the amplitudes corresponding to diagrams with n closed longitudinal photon loops behave like $(-1)^n[\Lambda^2/m_\gamma{}^2]^n/n!$. The strong Gaussian suppression in Eq. (6), $\exp\{-(\Lambda/m_\gamma)^2\}$, resulting from the delicate cancellation in the sum over loops, drastically "overkills" the second exponential factor in Eq. (6). In addition, since the result is so small, the inclusion of classes of diagrams, different from the bubbles considered, could drastically modify it.

Another amazing issue concerns the time scales. The photons emitted in the proposed processes are made very soft theoretically by the factor $(m_{\text{eff}}/m_\gamma)^{2/3} \approx 10^{-16}$ eV, corresponding to a lifetime of ~ 10 s. Thus it would appear that the filling of the K-shell model which takes place on the order of $\sim 10^{-14}$ s will occur before almost all of the soft photon emission, and hence cannot be affected by it. This issue has been raised by Okun and communicated to us [20].

The most important theoretical consideration, however, is that the search for charge violating decays is in fact a search for such radically "new physics" that even the Weinberg theorem might be violated. In particular, we could consider CV effects in connection with violations of energy-momentum conservation. In fact, charge and momentum are closely related in Kaluza-Klein or superstring models. In such models, charge is just the (angular) momentum corresponding to compactified higher dimensions. One of the presently advocated mechanisms suggested to explain the collapse of the wave function in quantum mechanics [21] also involves explicit, nonconventional energy, momentum, and unitarity violations. It is also possible that CV events might occur in conjunction with quantum gravity tunneling (wormhole effects) though admittedly no model of this type has been constructed to date. In these cases, the issues of CV decay rates and photon mass may no longer be coupled via the Weinberg theorem and each must be explored separately.

III. EXPERIMENTAL PROCEDURE

There are two channels for looking for electron decay in germanium detectors: either by searching for the spontaneous K-shell x rays generated by the decay $e^- \to \nu_e\nu_e\bar{\nu}_e$ or by looking for the decay of the electron into a neutrino and a 255 keV gamma, $e^- \to \nu_e\gamma$. In both types of searches, an ultralow background detector is needed for having any chance of detecting the possible decay signal from within the background in the corresponding energy regions. The lower the achieved background the more stringent the limit obtained for the lifetime of the above processes. The K-shell rays of the visible decay mode are difficult to measure even with a low background detector unless it has also a very low energy threshold. Consequently the searches for this decay mode are less frequent than for the neutrino-gamma decay channel.

After the pioneering work of Mateosian and Goldhaber [9] [$\tau(\nu_e\nu_e\bar{\nu}_e) > 10^{19}$ yr], followed by the limits obtained by Moe and Reines [4] [by using a NaI(Tl) detector] $\tau(\nu_e\nu_e\bar{\nu}_e) > 2 \times 10^{21}$ yr and $\tau(\nu_e\gamma) > 4 \times 10^{22}$ yr, and by Steinberg *et al.* [5], who first used a Ge detector for that purpose, $\tau(\nu_e\nu_e\bar{\nu}_e) > 5.3 \times 10^{21}$ yr, a new series of experimental efforts have been carried out in underground locations with very low background detectors and significantly tighter bounds have been obtained.

The experimental limits on these decays obtained in the past decade are grouped into two categories according to the detectors used. The results obtained with germanium spectrometers in underground locations are $\tau(\nu_e, \nu_e\bar{\nu}_e) > 2.9 \times 10^{22}$ yr [7], $2.7(1.7) \times 10^{23}$ yr [22] and $\tau(\nu_e\gamma) > 4.3 \times 10^{23}$ yr [7], 1.5×10^{25} yr [3], $2.35(1.19) \times 10^{25}$ yr [23], expressed at 68% (90%) confidence level. The second group corresponds to the search for K x-ray emission from iodine (binding energy=33.2 keV) in underground NaI detectors, which places the bounds $\tau(\nu_e\nu_e\bar{\nu}_e) > 0.2 \times 10^{23}$ yr [6], 1.2×10^{23} yr [24], 0.42×10^{23} yr [25] as well as to the searches for the specific channel $e^- \to \nu_e\gamma$ also with scintillators which provide $\tau(\nu_e\gamma) > 3.5 \times 10^{23}$ yr [6], 3.9×10^{23} yr [25].

The TWIN detectors consist in a set of two ~ 1.1 kg natural abundance germanium crystals mounted in specially constructed dipsticktype cryostats with two 90° bends separating the liquid nitrogen and cryopump material from the crystals. The germanium was specially deep mined; the final zone refinement and crystal growth were performed just prior to constructing the detectors and placing them underground. The copper cryostats were electroformed from a copper sulphate solution. The first-stage preamplifiers where shielded by 2.54 cm thick old lead pieces. The two germanium diodes of 1116 and 1105 g, respectively, had nominal dimensions of 65 mm in diameter and 67 mm in length. For further details on the electroforming copper cryostat process and on the germanium handling procedure see Ref. [26]. In order to minimize cosmogenic activation on the spectrometers, once finished they were driven directly and installed in the Homestake gold mine at a depth of 4000 m of water equivalent. They operated in the shielding configuration shown in Fig. 1 for a total effective exposure of 1.92 kg yr. Figure 2, which corresponds to the low energy data accu-

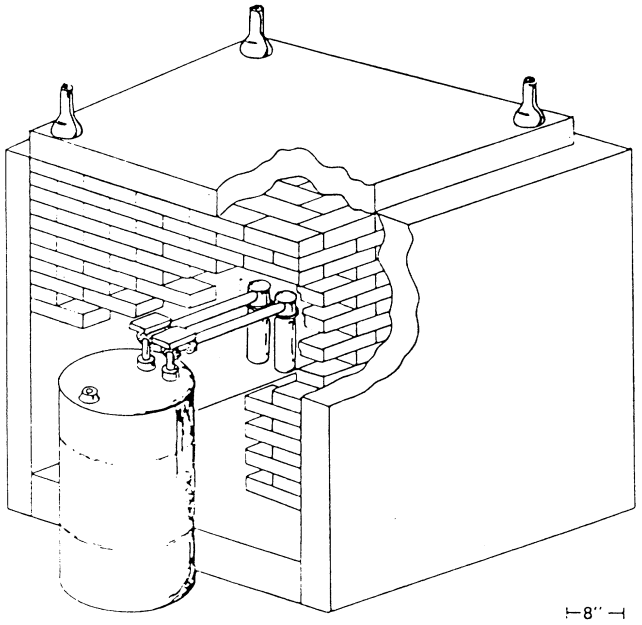

FIG. 1. Drawing of the experimental setup of the TWIN detectors.

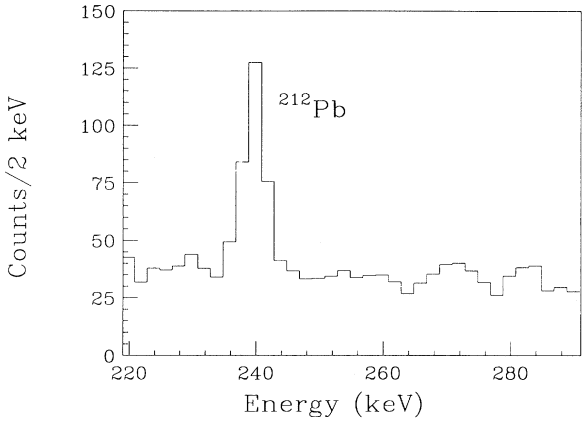

FIG. 3. Background spectrum of the TWIN detectors around the 255 keV region after 1.92 kg yr.

mulated during these 1.92 kg yr, shows the x-ray lines of copper and zinc cosmogenically induced on the detectors. Unlike the COSME detector described below, the poor instrumental resolution of the detectors does not allow to resolve these peaks. Figure 3 shows the background spectrum around the 255 keV region recorded with these detectors.

The COSME detector is a p-type coaxial hyperpure natural germanium crystal, of dimensions 22 mm (length)$\times$52.5 mm (diameter) corresponding to an active volume of 44 cm^3 and a mass of 253 g (including the dead layer) which has a long term resolution of 0.43 keV full width at half maximum (FWHM) at 10.37 keV and an energy threshold of 1.6 keV. The detector is also mounted in a dipsticktype electroformed copper cryostat (1.5 mm thick) and was built with ultralow background materials. The field effect transistor (FET) is shielded with 450-yr-old (Spanish) lead. Most of the techniques used in building the COSME detector follow closely those developed for the TWIN's. The detector is placed within a shielding of 10 cm of 2000-yr-old (roman) lead inner layer plus 20 cm of low activity lead (about 70 yrs old). A sheet of cadmium and 20 cm of paraffin and borated polyethylene complete the shielding. In order to avoid the vibrations transmitted to the detector and cryostat through the floor and through the experimental assembly, as well as to prevent airborne vibrations, all the shielding and mounting is supported by 10 cm of vibrational and acoustic insulator sandwiched within two layers of 10 cm of wood mounted on a floor of concrete (20 cm). Details of the experimental setup and parameters are given in Ref. [27]. A schematic view of the experimental setup is depicted in Fig. 4.

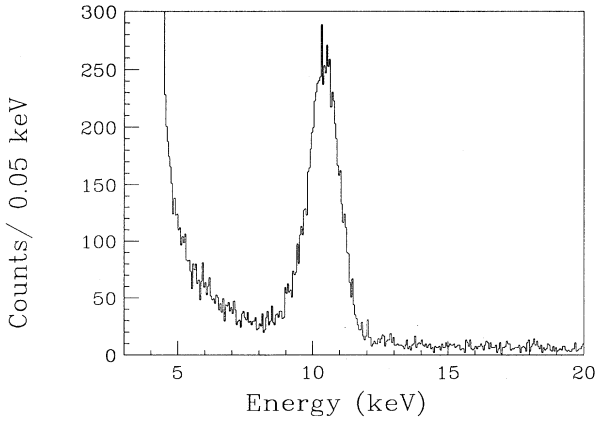

FIG. 2. The low energy region of the spectrum of the TWIN detectors after 1.92 kg yr of total effective exposure.

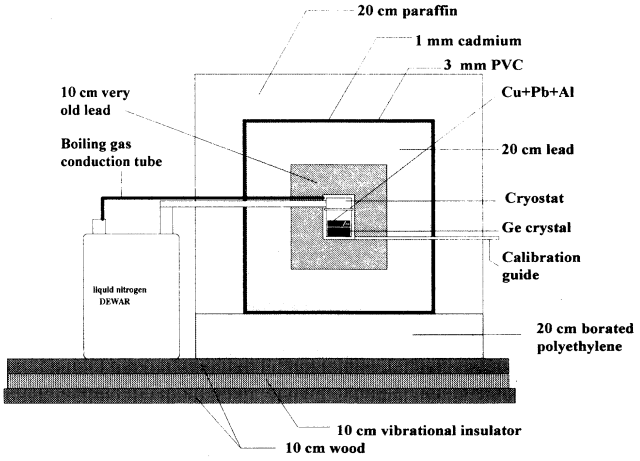

FIG. 4. Experimental setup used with the COSME detector.

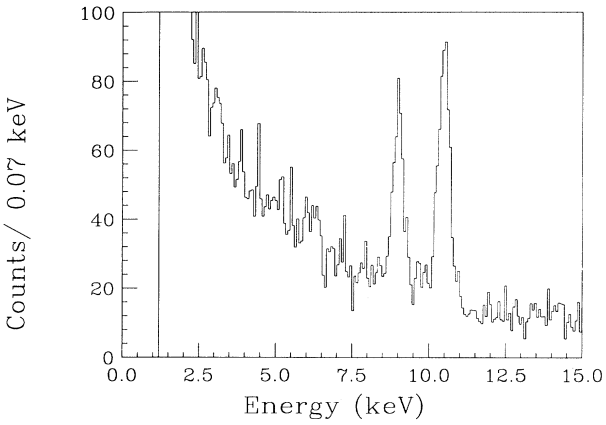

FIG. 5. The low energy region of the filtered spectrum obtained with the COSME detector after 130.7 kg d of effective exposure.

To improve the background and performances of the detector a method of filtering the microphonic noise based on the simultaneous use of two different shaping times in the processing of the signal, combined with the conventional time filtering process [22] of getting ride of those events not distributed evenly in time, has been developed. For details on the filtering procedures and on the complementarity and effectiveness of both methods see Ref. [27].

The filtered spectrum shown in Fig. 5 corresponds to an exposure of $Mt = 130.7$ kg d of COSME in the vicinity of the 11.1 keV region. Some peaks which clearly appear in the spectra are the Cu x ray (at 8.98 keV) and Ga x ray (at 10.37 keV) cosmogenically induced in the detector. Both x-ray peaks are clearly resolved and, obviously, not affected by the filtering procedures previously mentioned. Figure 6 shows the 255 keV energy region, recorded with the COSME detector for the same exposure.

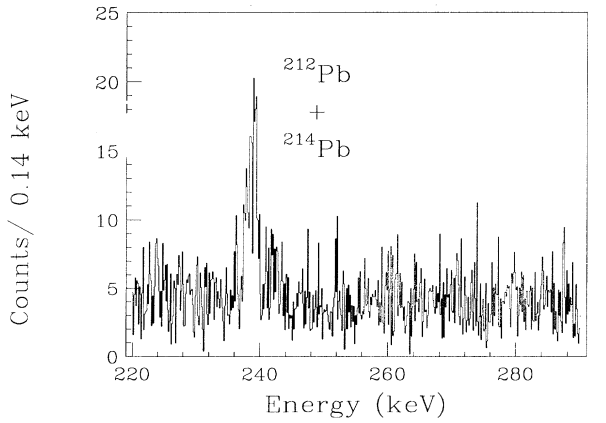

FIG. 6. View of the COSME spectrum in the 255 keV region for an exposure of 130.7 kg d.

IV. EXPERIMENTAL RESULTS

Because of the features (energy threshold, energy resolutions, and backgrounds) of each Ge detector we will use the data from TWIN to set lifetime limits for the decay mode $e^- \to \nu_e\gamma$, whereas COSME will be employed to obtain the lifetime bound in the $e^- \to \nu_e\nu_e\bar{\nu}_e$ decay search. The lower energy part of the spectrum is clearly resolved in COSME which features also a fairly low energy threshold. The TWIN, on the contrary, show a better background, in particular in the 255 keV energy region. In the case of the search for the $e^- \to \nu_e\gamma$ decay channel, the lower limit of the mean lifetime can be expressed as $\tau(\nu_e\gamma) > \sum \varepsilon_i N_i t/A$, where N_i stands for the number of electrons in the various components of the experimental device (Ge crystal, Cu cryostat, Pb shielding etc.) and ε_i represents the corresponding absolute peak detection efficiencies for the 255 keV γ ray. The quantity A is the maximum number of counts under the 255 keV peak (peak area) which could be attributed to the electron decay. Its value is obtained by means of standard statistical procedures (say a maximum likelihood method or a Poisson-with-background procedure [28]). The detector efficiencies were estimated through the EGS Monte Carlo simulation. The above expression, however, does not take into account the effect of the Doppler broadening on the decay of electrons in the different atomic shells [7]. Because of the average kinetic energy of the electrons in their orbital motion, the energy resolution of the detector is broadened from its nominal instrumental value. This effect is important for K- and L-shell electrons and should be also considered for M-shell electron decay. For instance, the decay of Cu K-shell (L-shell) electrons give a large Doppler width of $\sim$ 80 keV (27 keV) FWHM, causing their contribution to the 255 keV peak to be minimal.

The Doppler-broadened line shape has been calculated by assuming that the electrons have a temperature corresponding to the expectation value of the kinetic energy in a given energy level, which according to the virial theorem is $\langle E_{\rm kin}\rangle = -1/2\langle E_{\rm pot}\rangle$ for the Coulomb potential. The Doppler line shape is given as

$$I(E) = \frac{1}{\sqrt{2\pi}\sigma} \exp[-(E - E_0)^2/2\sigma^2] ,$$

where

$$\sigma = \sqrt{\frac{KT}{m_e c^2}} E_0 = \sqrt{\frac{E_B}{m_e c^2}} E_0 ,$$

with K the Boltzmann constant, T the absolute electron temperature, m_e the electron mass, and E_0 the γ-ray energy from the decay of the electron in a given level. E_B is the absolute value of the electron binding energy:

$$E_0 = \frac{m_e c^2 - E_B}{2} .$$

As there are various different subshells involved for the Ge, Cu, and Pb electrons which may decay, a sum of different Gaussian lines contributes to the line shape:

$$\sum_{i=1}^{29} \frac{1}{\sqrt{2\pi}\sigma_i} \exp[-(E-E_{0i})^2/2\sigma_i^2]\varepsilon_{\mathrm{Cu}} N_{\mathrm{at}}(\mathrm{Cu})$$

$$+\sum_{i=1}^{32} \frac{1}{\sqrt{2\pi}\sigma_i} \exp[-(E-E_{0i})^2/2\sigma_i^2]\varepsilon_{\mathrm{Ge}} N_{\mathrm{at}}(\mathrm{Ge})$$

$$+\sum_{i=1}^{82} \frac{1}{\sqrt{2\pi}\sigma_i} \exp[-(E-E_{0i})^2/2\sigma_i^2]\varepsilon_{\mathrm{Pb}} N_{\mathrm{at}}(\mathrm{Pb}) \ .$$

In the case of the COSME detector the number of Ge atoms, including the dead layer, is $N_{\mathrm{at}}(\mathrm{Ge}) = 2.10 \times 10^{24}$ atoms. The Cu cryostat has dimensions 7.6 cm in diameter by 24.75 cm in length, with a thickness of 1.5 mm and so $N_{\mathrm{at}}(\mathrm{Cu}) = 8.45 \times 10^{24}$. The volume of the COSME lead shielding is $70 \times 70 \times 70$ cm^3 with an inner cavity of $10 \times 10 \times 30$ cm^3, and so the number of lead atoms $N_{\mathrm{at}}(\mathrm{Pb}) = 1.45 \times 10^{28}$. As far as the absolute peak detection efficiencies for 255 keV γ rays, one has for the COSME detector $\varepsilon_{\mathrm{Ge}} = 0.16$, $\varepsilon_{\mathrm{Cu}} = 4.1 \times 10^{-3}$, and $\varepsilon_{\mathrm{Pb}} = 5.3 \times 10^{-6}$ for electron's emission in Ge (dead zone included), in the Cu cryostat and in the Pb shielding, respectively. The instrumental detector resolution at 255 keV, $\Gamma_{\mathrm{FWHM}} = 1.8$ keV, rises up to 5.3 keV due to the Doppler broadening. A maximum likelihood analysis was performed to get the upper limit of the peak area A. The average background at the $E = 255.5$ keV energy region is 28.7 $c\,\mathrm{keV}^{-1}$ in 13 404 h of statistical time. The maximum number of counts under the 255.5 keV Doppler-broadened electron decay peak is 15.8 (28.6), leading to mean life lower limits of $\tau(\nu_e\gamma) > 1.7(0.97) \times 10^{24}$ yr, 68%(90%) C.L.

When a similar analysis is performed with the data from the TWIN detectors, the electron lifetime lower limits obtained for the $e^- \to \nu_e\gamma$ decay mode are one order of magnitude more stringent than those of COSME because of its better background. In this experiment, the background is $B(\sim 255\ \mathrm{keV}) = 8.8\ c\,\mathrm{keV}^{-1}\,\mathrm{kg}^{-1}\,\mathrm{yr}^{-1}$ (see Fig. 3); the number of atoms and absolute peak efficiencies, defined as above, are $N_{\mathrm{at}}(\mathrm{Ge}) = 8.78 \times 10^{24}$ (for each TWIN detector), $N_{\mathrm{at}}(\mathrm{Cu}) = 8.5 \times 10^{24}$, $N_{\mathrm{at}}(\mathrm{Pb}) = 8.13 \times 10^{25}$ and $\varepsilon_{\mathrm{Ge}} = 0.66$, $\varepsilon_{\mathrm{Cu}} = 0.04$, and $\varepsilon_{\mathrm{Pb}} = 2.9 \times 10^{-3}$. In this analysis the contribution from Pb atoms residing deeper than 0.61 cm into the internal cavity surrounding the detectors has been neglected, due to the total screening of a 255.5 keV gamma originating beyond that layer. The detector resolution at 255 keV, $\Gamma_{\mathrm{FWHM}} = 3.9$ keV, rises up to 11.2 keV after Doppler broadening is included. A maximum likelihood analysis of the region 220–280 keV gives a maximum number of counts under the 255.5 keV Doppler broadened peak of 10.6 (19.0) at 68% (90%) confidence level. This in turn leads to a mean life lower limit of

$$\tau(\nu_e\gamma) > 3.7(2.1) \times 10^{25}\ \mathrm{yr}\ 68\%(90\%)\ \mathrm{C.L.},$$

which improves the best previously published limits [23].

Another more general method to test the electron stability is to search for the "invisible" decay $e^- \to \nu_e\nu_e\bar{\nu}_e$.

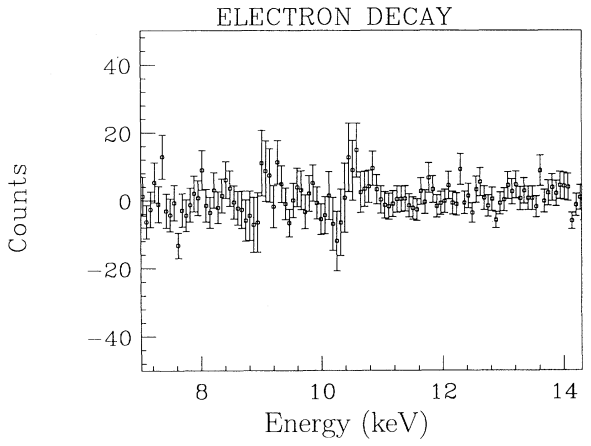

FIG. 7. The low energy region spectrum of COSME after subtraction of the best fit function.

The decay of a K-shell electron will leave a hole and the consequent x-ray cascade will result in a peak of 11.1 keV (binding energy of an $1s$ electron in Ge). These x rays are difficult to measure, even with low background detectors. The current limits stand at levels two orders of magnitude less stringent than the bounds obtained through the less general, specific channel $e^- \to \nu_e\gamma$. As stressed above the good energy resolution of COSME allows us to resolve the 11.1 keV peak from the other x-ray peak in that region (Cu x-ray peak at 8.98 keV, Zn x-ray peak at 9.66 keV, and Ga x-ray peak at 10.37 keV). Furthermore, the fairly good background of COSME in that region (5 to ~15 keV) allows us to extract, in conclusion, better mean life lower limits than those reported up to now.

We obtain the mean life lower limit by using the ex-

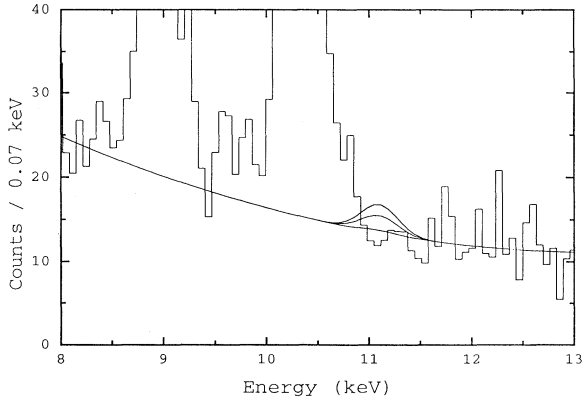

FIG. 8. Region of interest for the electron decay in the spectrum obtained with the COSME detector after 130.7 kg d of effective exposure. The curves correspond to the best fit, 68% C.L. and 90% C.L. compatible excess counts assuming Gaussian peak shapes.

TABLE I. Comparison of the fits with different analytical functions.

Peak shape function	8.98 keV area Main Gaussian	Lower tail	Upper tail	Total	10.37 keV area Main Gaussian	Lower tail	Upper tail	Total	χ^2	ν	11.1 keV area	A 68(90%) C.L.
$F1$	321			321	491			491	140.6	133	2 ± 13	13.8(22.7)
$F2$	316			316	489			489	146.1	128	4 ± 11	13.0(20.7)
$F3$	297	28		325	438	57		495	135.9	123	0 ± 12	12.0(19.7)
$F4$	286	22	19	327	422	55	20	497	143.5	113	3 ± 14	15.3(24.8)

pression $\tau(\nu_e\nu_e\bar{\nu}_e) > N_1\varepsilon_1 t/A$. Here $N_1 = 2\times2.1\times10^{24}$ is the number of K electrons in Ge quoted above, $t = 13\,404$ h is the running time for the COSME spectrum, and the peak efficiency for the 11.1 keV x rays emitted anywhere in the germanium crystal (dead layer included) is given by $\varepsilon_1 = 0.93$. The background in the 11.1 keV energy region is 1.6 $c\,\mathrm{keV}^{-1}\,\mathrm{kg}^{-1}\,d^{-1}$. The upper limit to the number of counts under the 11.1 keV peak, A, is determined by fitting four Gaussians and a second order polynomial to the experimental spectrum in the region from 5 to 15 keV. The Gaussian centroids are fixed at the values $E_a = 11.1$ keV, $E_b = 10.37$ keV, $E_c = 9.66$ keV, and $E_d = 8.98$ keV, and their widths at $\sigma_a = 0.20$ keV, $\sigma_b = 0.19$ keV, $\sigma_c = 0.18$ keV, and $\sigma_d = 0.17$ keV. This fit (see Fig. 7) yields the areas $A_a = 2\pm13$, $A_b = 491\pm27$, $A_c = 43 \pm 16$, and $A_d = 321 \pm 24$, and therefore a maximum number of 11.1 keV x rays $A = 13.8$ (22.7) at 68% (90%) C.L.(see Fig. 8). The corresponding electron lifetime lower limit so obtained is

$$\tau(\nu_e\nu_e\bar{\nu}_e) > 4.3(2.6) \times 10^{23} \text{ yr } 68\%(90\%) \text{ C.L.}$$

This value represents an improvement of a factor 1.5 over the previous best value obtained with Ge detectors [22], and of a factor 3.5 with respect to the bests limit from K-electron decay in NaI detectors [24].

Since the upper limit of the number of counts under the 11.1 keV peak area can be sensitively dependent on the shape assumed to fit the neighboring 10.37 keV x-ray peak, we have estimated the systematic errors which could be introduced by the arbitrary choice of a Gaussian function to describe the peaks on a germanium detector. As we will show that choice does not essentially affect the results presented in this paper.

To prove this statement we have fitted the above mentioned peaks to several commonly used analytical functions. Table I gives the main peak area in the low energy spectral region obtained with the various fitting functions employed. $F1$ denotes the fit used in the estimate of the electron lifetime lower limit derived above. $F2$ stands for a fit on which a steplike Gaussian broadened function $p_0\mathrm{erfc}[(E - E_0)/2^{1/2}\sigma]$ has been added in the description of the spectral background shape. On $F3$ a lower exponential function $p_1\exp(p_2y)/[1 + \exp(y)]^4$, where $y = (E - E_0)/\sigma$, has been introduced to represent the low-energy tailing of the Gaussian peaks. And finally, $F4$ besides the lower exponential function includes a higher exponential function $p_3\exp(p_4y)/[1+\exp(-y)]^4$ to account for possible high-energy tailings on the peaks. All fits were performed with a background function described by a second order polynomial.

The contribution of the tails to the total peak areas are detailed, being always smaller than 15% of the total area and, in particular, the higher-energy tailings are at most 6%. The χ^2, weighted with $\sigma^2 = c$, where c are the number of counts on each channel, obtained in the fits and the degrees of freedom (ν) for each analytic fit are also shown in order to allow comparison of the quality of the fits. The total area of the peak of 8.98 keV has a range of 3.4% (from 316 to 327) and that of the 10.37 keV peak has a range of 1.6% (from 489 to 497). The small differences on the χ^2 and on the peak areas estimates indicate that the choice of the peak shape function is not crucial on the limits on the electron lifetime presented in this work. The table also shows the estimates of the 11.1 keV peak area and the upper limits (A) on the number of counts under the peak derived from these procedures.

ACKNOWLEDGMENTS

This work was supported by the National Science Foundation under Grant No. PHY-9007847 and by CICYT (Spain) and Diputación General de Aragón. The Canfranc Underground Laboratory is operated by the Institute of Nuclear and High Energy Physics of the University of Zaragoza. The Pacific Northwest Laboratory is operated for the U.S. Department of Energy by Battelle Memorial Institute under Contract No. DE-AC06-76RLO 1830. We thank R. Núñez-Lagos for his collaboration in the mounting of the shielding of the COSME experiment.

[1] H. Georgi and S. L. Glashow, Phys. Rev. Lett. **32**, 438 (1974).
[2] H. Primakoff and S. P. Rosen, Annu. Rev. Nucl. Part. Sci. **31**, 145 (1981).
[3] F. T. Avignone III, R. L. Brodzinski, W. K. Hensley, H. S. Miley, and J. H. Reeves, Phys. Rev. D **34**, 97 (1986).
[4] M. K. Moe and F. Reines, Phys. Rev. **140**, 992 (1965).
[5] R. I. Steinberg, K. Kwiatowski, W. Maenhout, and N. S. Wall, Phys. Rev. D **12**, 2582 (1975).
[6] E. L. Kovalchuk, A. A. Pomanski, and A. A. Smolnikov, Pis'ma Zh. Eksp. Teor. Fiz. **29**, 163 (1979) [JETP Lett. **29**, 145 (1979)].

[7] E. Bellotti, M. Corti, E. Fiorini, C. Liguori, A. Pullia, A. Saracino, P. Sverzellati, and L. Zanotti, Phys. Lett. **124B**, 435 (1983).
[8] F. Reines and H. W. Sobel, Phys. Rev. Lett. **32**, 954 (1974).
[9] G. Feinberg and M. Goldhaber, Proc. Natl. Acad. Sci. U.S.A. **45**, 1301 (1959).
[10] A. Y. Ignatiev, V. A. Kuzmin, and M. E. Shaposhnikov, Phys. Lett. **84B**, 315 (1979).
[11] M. B. Voloshin and L. B. Okun, Pis'ma Zh. Eksp. Teor. Fiz. **28**, 156 (1978) [JETP Lett. **28**, 145 (1978)].
[12] L. B. Okun, *Leptons and Quarks* (North-Holland, Amsterdam, 1982), p. 181.
[13] L. B. Okun and Y. B. Zeldovich, ITEP Report No. 79, 1978 (unpublished).
[14] L. B. Okun and Y. B. Zeldovich, Phys. Lett. **78B**, 579 (1978).
[15] L. B. Okun, Comments Nucl. Part. Phys. **19**, 99 (1989); Usp. Fiz. Nauk **158**, 293 (1989); in Particle Data Group, K. Hikasa *et al.*, Phys. Rev. D **45**, S1 (1992), p. V1.10.
[16] M. Suzuki, Phys. Rev. Lett. **56**, 1339 (1986).
[17] M. M. Tsypin, Sov. J. Nucl. Phys. **50**, 269 (1989) [Yad. Fiz. **50**, 431 (1989)].
[18] S. Weinberg, Phys. Rev. **135**, B1049 (1964).
[19] A. S. Goldhaber and M. M. Nieto, Rev. Mod. Phys. **43**, 277 (1971).
[20] S. Nussinov (private communication).
[21] G. C. Ghirardi, A. Rimini, and T. Weber (private communication).
[22] D. Reusser, M. Treichel, F. Boehm, C. Broggini, P. Fisher, L. Fluri, K. Gabathuler, H. Herikson, V. Jörgens, L. W. Mitchell, C. Nussbaum, and J. L. Vuilleumier, Phys. Lett. B **255**, 143 (1991).
[23] A. Balysh, M. Beck, S. Belyaev, F. Bensch, J. Bockholt, A. Demehin, A. Gurov, G. Heusser, H. V. Klapdor-Kleingrothaus, I. Kondratenko, V. Lebedev, B. Maier, A. Müller, F. Petry, A. Piepke, H. Strecker, and K. Zuber, Phys. Lett. B **298**, 278 (1993).
[24] H. Ejiri, H. Kinoshita, H. Sano, and H. Ohsumi, Phys. Lett. B **282**, 281 (1992).
[25] M. L. Sarsa *et al.* (unpublished).
[26] R. L. Brodzinski, H. S. Miley, J. H. Reeves, and F. T. Avignone III, Nucl. Instrum. Methods A **292**, 337 (1990); H. S. Miley, F. T. Avignone III, R. L. Brodzinski, J. I. Collar, and J. H. Reeves, Phys. Rev. Lett. **65**, 3092 (1990).
[27] J. Morales, E. García, A. Ortiz de Solorzano, A. Morales, R. Núñez-Lagos, J. Puimedón, C. Sáenz, and J. A. Villar, Nucl. Instrum. Methods A **321**, 410 (1992).
[28] Particle Data Group, L. Montanet *et al.*, Phys. Rev. D **50**, 1173 (1994).